# iet

# Determining the envelope of the blood flow velocity in Doppler ultrasound

Jarosław Majewski, Krzysztof J. Opieliński, Paweł Żogał, and Andrzej Wiktorowicz

Abstract—This paper describes and tests a method for automatically determining the envelope of the blood flow velocity curve in ultrasonic Doppler imaging, which was implemented in a prototype of the 128-channel mobile ultrasound B-mode scanner. On the basis of the determined envelopes, algorithms were also developed for the automatic determination of the most important characteristic points of the Doppler blood flow spectrum in pulse wave Doppler imaging mode and the most relevant blood flow parameters. Sufficiently good repeatability and precision were obtained with low computational complexity.

Keywords—spectral Doppler ultrasound; Color Flow Mapping (CFM); Pulsed Wave Doppler (PWD); blood flow velocity envelope; blood flow pulsation indices

#### I. Introduction

PECTRAL Doppler ultrasound imaging is one of the basic methods for the diagnosis of vascular disease, as it allows the location and evaluation of the extent of atherosclerotic lesions [1]. Blood flow velocity is recorded in the form of a Doppler spectrum, from which the envelope of instantaneous maximum and minimum blood flow velocity is determined, as well as pulsation and flow resistance indices - characteristic quantities indicating progressive changes in blood vessels. The accuracy of determining these parameters is significantly influenced by the accuracy of determining the envelope and characteristic points of the Doppler blood flow waveform.

In the framework of the present work, a method was developed for the automatic determination of the envelope of the blood flow velocity curve in spectral Doppler imaging. It is characterised by sufficiently good repeatability and precision, as well as low computational complexity, so that the envelope can be determined and displayed on the fly during *in vivo* measurements. The developed method has been implemented in a prototype of the 128-channel mobile ultrasound B-mode scanner (Fig. 1), along with enhanced imaging methods that increase the functionality of the device and enable better quality images of tissues examined *in vivo* (both in diagnostic medical and veterinary applications) with high spatial resolution, contrast, reduction of acoustic noise, multiple reflections, and acoustic shadows, with the ability to mark elastic properties of tissues and options for determining their numerical parameters.

To this end, in addition to Doppler imaging of blood flow in blood vessels, the prototype was equipped with a number of

The research described in the paper was carried out as part of the POIR.01.01.01-00-1462/19 research project funded by the National Centre for Research and Development (NCBR) with funds from the European Union.

J. Majewski and A. Wiktorowicz are with DRAMINSKI S.A., Poland (e-mails: jareks@draminski.com, andrzej.wiktorowicz@draminski.com).

other advanced methods of ultrasound imaging and tissue characterisation: Tissue Harmonic Imaging (THI), image composition for several beam deflection angles (Compound Imaging (CI)), 3D imaging reconstructed from standard 2D images acquired during manual movement or rotation of the ultrasonic probe, compression elastography, Coded Ultrasound (CU), an algorithm for contour detection of hypoechoic areas and the ability to determine their basic geometric parameters (circumference, area, rotational volume). The prototype has also been equipped with a telemedicine option to transmit ultrasound images and control the device remotely, e.g. from a tablet, smartphone or computer.



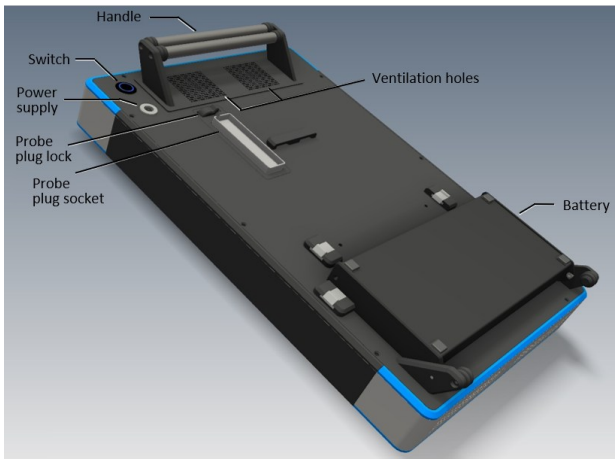


Fig. 1. A view of the developed prototype of the 128-channel mobile ultrasound scanner with expanded imaging methods.

- K.J. Opieliński is with Department of Acoustics, Multimedia and Signal Processing, Faculty of Electronics, Photonics and Microsystems, Wrocław University of Science and Technology, Poland (e-mail: krzysztof.opielinski@pwr.edu.pl).
  - P. Żogał is with CYBERMEDICS, Poland (e-mail: pzogal@cybermedics.pl).



#### II. DESCRIPTION OF THE METHOD

Blood flow velocity is recorded in the form of a Doppler spectrum (Fig. 2), from which the envelope of instantaneous maximum and minimum blood flow velocity is determined, as well as pulsation and flow resistance indices - characteristic quantities indicating progressive atherosclerotic changes in blood vessels. Figure 2 shows an example of blood flow velocity spectrum of the brachial artery of a human upper limb phantom, obtained using a SmartUs ultrasound B-mode scanner from Telemed and Pulsed Wave Doppler (PWD) mode (Fig. 3). The phantom was powered by flow using a Doppler Flow Pump Model 769 peristaltic pump [2]. The human upper limb phantom was filled with Doppler Fluid Model 769DF to mimic blood [3].

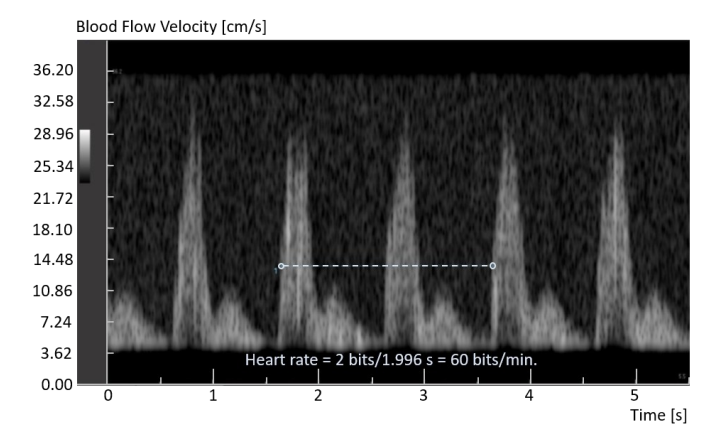


Fig. 2. An example of blood flow velocity spectrum of the brachial artery of a human upper limb phantom obtained using a SmartUs ultrasound B-mode scanner from Telemed with PWD mode.



Fig. 3. Laboratory test blood flow velocity measurement system of a human upper limb phantom supplied with the Doppler Fluid Model 769DF [3] using the Doppler Flow Pump Model 769 [2].

The Doppler phenomenon describes the change in frequency of an acoustic (or electromagnetic) wave depending on the movement of the wave source and the point of the receiver. If the source of the wave moves toward the observer, the wavelength shortens, and the frequency increases. On the other hand, if the source moves away, the wavelength lengthens and the frequency decreases. This method is used in many fields, including medicine, to help diagnose diseases such as heart disease and vascular disease. This uses an ultrasound wave that is reflected by erythrocytes in the blood that flows through the veins and arteries (Fig. 4). The speed of blood flow and abnormalities in the circulatory system can be determined by changes in the frequency of the ultrasound wave, which are caused by the movement of erythrocytes [1],[4].

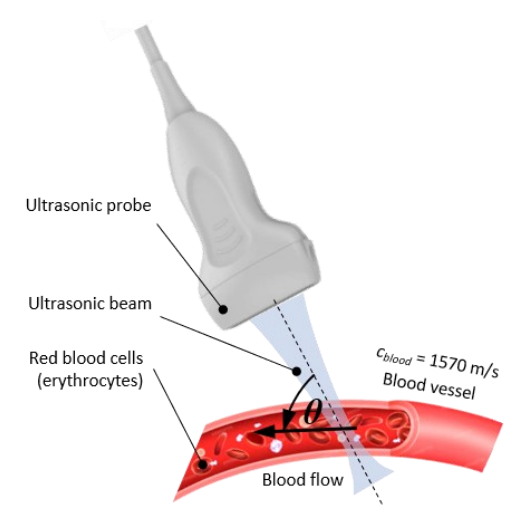


Fig. 4. Illustration of the ultrasonic measurement method of blood flow velocity using the Doppler phenomenon.

Ultrasound waves, scattered on blood cells that flow in blood vessels, change their frequency by the so-called Doppler shift  $f_D$ . The transducer, which acts as a transmitter, emits an ultrasound wave of frequency  $f_T$ , after which a reflected wave of frequency  $f_R$  reaches the receiver. The frequency shift  $f_D$  recorded on the transducers is analysed:

$$f_R = f_T \pm f_D \tag{1}$$

where the  $\pm$  sign corresponds to the direction of blood flow relative to the transducers [1]. The Doppler frequency is determined by these changes, taking into account the angle of movement of the blood cells relative to the emitted beam (Fig. 4) using the formula:

$$f_D = \pm 2 \frac{V}{c} f_T \cos \theta \tag{2}$$

where V is the velocity of blood flow in the blood vessel,  $\theta$  is the angle between the axis of the ultrasound beam and the axis of the blood vessel (Fig. 4), while c is the speed of propagation of the ultrasound wave in the blood (1570 m/s). It follows that if the blood cells flow in the direction towards the source, the frequency of the reflected wave is higher than the transmitted one, while the opposite effect occurs as the blood cells move away. The correct estimation of the angle  $\theta$  has a significant impact on the accuracy of the Doppler frequency  $f_D$ measurement, which is reflected in the speed of the measured flow. A larger deviation generates a larger measurement error. Therefore, it is very important to correctly operate the ultrasound transducer when measuring. The Doppler shift  $f_D$  in blood flow measurements has a wide spectrum, from frequencies close to zero for blood cells that flow slowly near the walls to maximum values for those flowing in the centre of the vessel. The highest detection sensitivity occurs at the intersection of the ultrasound transmit and receive beams.

Finally, after transformations, the formula that allows the conversion of Doppler frequency to blood flow velocity can be written in the following form:

$$V\left[\frac{\text{cm}}{\text{s}}\right] = \pm 78.5 \cdot \frac{f_D \text{ [kHz]}}{f_T \text{ [MHz]}} \cdot \frac{1}{\cos \theta}$$
 (3)

# A. Calculation of the Blood Flow Velocity Spectrum

A method based on Short-Time Fourier Transform (STFT) analysis with filtering using window filters [5],[6] was used to calculate the blood flow velocity spectrum (the so-called

Doppler blood flow waveform). The STFT method involves traversing a time window of a given length (the number of samples usually being a power of number 2) with a certain step along a Doppler signal (a filtered differential signal containing Doppler frequencies) and analysing the frequency composition of such a signal in each window. In conventional digital signal processing applications, the STFT is often determined only in a finite set of evenly spaced points along the frequency axis (similar to the Discrete Fourier Transform (DFT) instead of the Discrete-Time Fourier Transform (DTFT)):

$$X(n,k) = \sum_{m=n-(N_W-1)}^{n} w(n-m) \cdot x(m) e^{-j2\pi mk/N}$$
 (4)

or

$$X(n,\omega_k) = \sum_{m=n-(N_W-1)}^n w(n-m) \cdot x(m) e^{-j\omega_k m}$$
 (5)

where x(n) - discrete Doppler signal defined for all n, w(n) - window of finite duration with non-zero values of n from 0 to  $N_w - 1$ , N - the number of discrete frequency channels used in STFT,  $N_w$  - length of window function. Using such notational conventions, the frequencies for which the STFT is calculated are defined as  $\omega_k = 2\pi k/N$ . The function X(n,k) is a function of both time and frequency, and the time and frequency variables are discrete. The variable n denotes the position of the analysis window along the time axis, and the segment of time bounded by the window is often called the analysis frame. The variable k, on the other hand, is a frequency index and is often referred to as a "frequency bin":

$$k = n \cdot \frac{f_s}{N} = \frac{n}{N \cdot \Delta t_s} \tag{6}$$

where n = 0, ..., N-1, N - DFT length,  $f_s$  - sampling frequency,  $\Delta t_s = 1/f_s$ . The number of bins is directly related to the width of the DFT size, and the bin (also called line spacing) determines the frequency resolution. The number of bins in an FFT is generally half the FFT size (N/2). Referring to the definitions presented here in equation (4) and (5), we can think of the STFT as representing the DFT of the finite-duration time function  $x(m) \cdot w(n-m)$ . In this context, the variable m is a dummy time argument, while the variable n identifies the location of the short segment of the original time function as it is extracted using the window w(n-m), which moves along the m-axis according to the value of n. In general, STFT can be defined in terms of the output of any filter bank [9]. In Equations (4) and (5), however, we limit ourselves to the simplest case of identical symmetric bandpass filters of equal frequency. The result of these simplifications is to allow the use of a single low-pass filter in the form of a window function w(n), which determines all the properties of the filter bank.

From a qualitative point of view, the STFT can be defined as a set of fast Fourier transforms (FFTs) performed on overlapping time segments in which the signal has been previously divided by a window translation (e.g., Hamming, Hanning) in time (Fig. 5). To apply the FFT, the length of the time window is chosen short enough to guarantee the pseudo-stationarity hypothesis for each signal segment. In this way, STFT is computationally efficient and allows analysing the Doppler signal spectrum during *in vivo* blood vessel flow studies.

Note that the length of the time window affects both the time resolution and the frequency resolution of the STFT. A narrow window results in high temporal resolution but coarse frequency resolution because it has a short duration but wide frequency bandwidth. A wide window results in high frequency resolution but coarse time resolution because it has a long duration but narrow frequency bandwidth. This phenomenon is called the window effect. With STFT, high time and frequency resolution cannot be achieved simultaneously. In the case of a time-invariant window, the STFT has the same time and frequency resolution in the entire time-frequency plane.

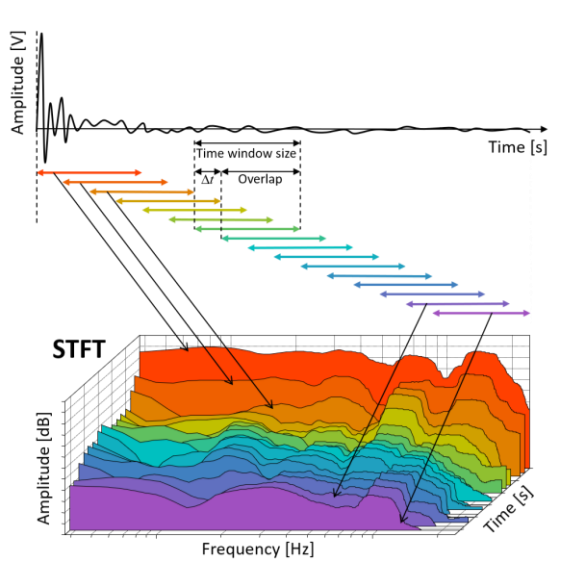


Fig. 5. Illustration of a method based on short-time Fourier transform (STFT) analysis.

The optimal choice of window length depends on the characteristics of the signal being analysed. The window length should be small enough so that the windowed signal block is essentially stationary within the window interval, and large enough so that the Fourier transform of the windowed signal block provides reasonable frequency resolution. If the spectral content of the signal changes slowly over time, which does not require exact time resolution, set the window wide. If the spectral content of the signal changes relatively fast, which requires accurate time resolution, set a narrow window. The time window can be moved over the analysed signal with or without overlap. Overlapping the sliding window makes the STFT smoother along the time axis, but this requires more computing time and memory resources. If the signal length is large and the spectral content in the signal changes slowly, no overlay is necessary. If the signal length is small, overlaying should be used to obtain a smoother STFT spectrum. An alternative solution is to use overlapping windows and add samples with zero values at the end window edges (zero padding technique) to increase the time and frequency resolution.

# B. Determination of the Envelope

Figure 6 shows an example of a 3D Doppler frequency spectrum showing the distribution of individual Doppler shifts (amplitudes), flow directions (above and below the time axis) and flow velocities calculated from Doppler frequency shifts (equation (3)) [1]. This spectrum is usually plotted in the form of a two-dimensional histogram (Fig. 2). The vertical axis in the plane of the graph represents different flow velocities over time (horizontal axis) as Doppler frequency shifts. The amplitude on the vertical axis perpendicular to the plane of the graph represents the number of red blood cells moving at a specific

velocity (varying brightness levels in a two-dimensional histogram). The flow in the direction to and from the ultrasound transducer is processed simultaneously and represented above and below the baseline (zero flow velocity line - blue belt in Fig. 6), respectively.

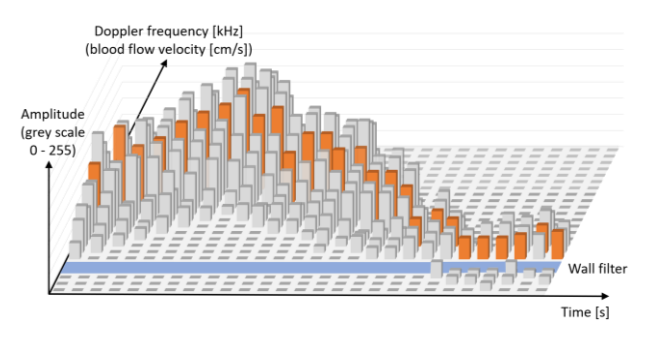


Fig. 6. An example of a three-dimensional Doppler frequency spectrum [1].

To eliminate interfering signals from the Doppler spectrum, a high-pass wall filter is used to eliminate low-frequency noise artefacts caused by slow flow and vascular wall motion artefacts from the frequency spectrum. Most wall filters have a cutoff range of 100 - 400 Hz [1]. More sophisticated filters eliminate only low frequencies of high amplitude (typical of wall motion) or identify and eliminate typical tissue motion patterns. The orange coloured amplitude bars of Doppler frequencies in Fig. 6 correspond to mean blood flow velocities determined by averaging the amplitudes over time intervals [10]. However, the waveform (envelope) of mean blood flow over time determined in this way is often falsified because of the averaging of various noise, which does not represent the movement of blood cells. In addition, the mean flow velocity can be erroneously determined here if slow flow components with low Doppler shifts have also been filtered out along with noise. The accuracy of determining the envelope and characteristic points of the Doppler blood flow waveform has a significant impact on the accuracy of determining characteristic diagnostic parameters (pulsation index and flow resistance) indicative of progressive changes in blood vessels. It should be noted that manufacturers of ultrasound B-mode scanners in which such functionality is implemented do not disclose the developed method of determining the spectral envelope.

For determining the maximum and minimum envelope of the Doppler frequency spectrum (Fig. 2, Fig. 6), the standard algorithms used to determine the envelope of acoustic signals (such as the Hilbert transform) are not suitable, due to the width of the spectrum and blurring its edges at particular time segments (Fig. 5). The authors began their work on this issue by analysing the possibility of testing the efficiency of signal-tonoise transitions using the sum of gradients when traversing the envelope path, as well as the possibility of using the SSA method (Singular Spectrum Analysis) [11]. After testing the SSA method, it was found to be well suited to the continuous component of the spectrum and very low-frequency components; it is computationally very complex and does not give conclusive results when determining the envelope of the Doppler spectrum. Not-satisfied results were also obtained using image filtering (e.g. edge filters). After preliminary studies, it was concluded that the quick determination of the instantaneous envelope of the temporal Doppler spectrum should be based on an easy statistical analysis of the image pixel

values in the form of a two-dimensional histogram (Fig. 2). As a result, a novel method for automatic determination of instantaneous envelopes of the temporal waveform of the Doppler spectrum was developed and successfully implemented and tested in the present work, which is based on the selection of a threshold parameter of the values of the searched image pixels in grey shades (two-dimensional histogram as in Fig. 2) using analysis of variance. The Doppler spectrum envelope determination algorithm works by sequentially searching the pixel values in all N vertical lines of the two-dimensional spectrum histogram (Fig. 2), for different increasing thresholds of the Th values of image pixels. In this way, a maximum of 256 envelopes of the Doppler spectrum  $V_{Th}(t)$  in each time frame of the greyscale display image are determined. Each envelope is determined for the intensity of the pixels in the vertical lines of the image corresponding sequentially to individual or selected ranges of threshold values from 0 to 255 (e.g.,  $Th \ge 0$ ,  $Th \ge 1$ , ...,  $Th \ge 255$ ). The algorithm allows us to determine the envelope of maximum instantaneous velocities (Max - red colour) as a result of searching the pixels of vertical image lines from the top and minimum (Min - green colour) as a result of searching the pixels of vertical image lines from the bottom. Then an optimal upper envelope (Max) and one lower envelope (Min) (Fig. 7) are selected based on the criterion of minimum variance  $S^{2}(V_{Th}(t))$ , calculated using the formula:

$$S^{2}(V_{Th}(t)) = \frac{\sum_{i=1}^{N} (v_{Th_{i}} - \overline{v_{Th}})^{2}}{N-1}$$
 (7)

where  $V_{Th}(t)$  – the envelope of the Doppler spectrum waveform in the time frame of the image displayed in greyscale for the pixel intensities corresponding to Th threshold values, N - the number of points of the envelope over time equals the number of pixels of the image horizontally (i.e., the number of vertical lines of the image),  $\overline{V_{Th}}$  – the average value of the image points of each envelope  $V_{Th}(t)$ :

$$\overline{V_{Th}} = \frac{\sum_{i=1}^{N} v_{Th_i}}{N} \tag{8}$$

where  $V_{Th_i}$  – the *i* value of the envelope point  $V_{Th}(t)$ , while i = 1, 2, ..., N.

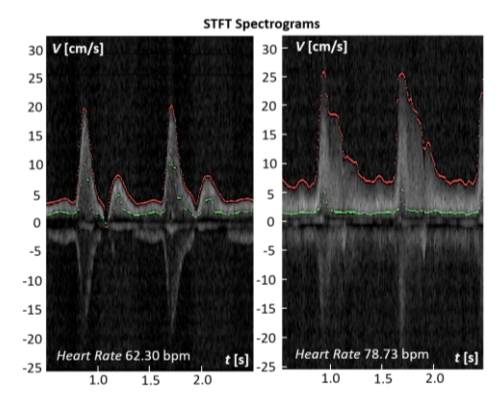


Fig. 7. Example results of the algorithm developed for automatic calculation of the blood flow velocity spectrum envelope (STFT spectrograms).

Both envelopes can be determined in one of three modes: lower, upper, or both halves of the velocity spectrum. In the latter case, the envelope is determined for only one half of the Doppler spectrum at a time, i.e. for blood flow in one direction (Fig. 7). The selection of the half is done automatically by the algorithm

based on the statistical distribution of the velocity spectrum calculated for both halves. The choice of modes is made by the operator. The envelope determination algorithm additionally developed two options for envelope smoothness settings, LOW and HIGH (Fig. 8) realised by averaging filters.

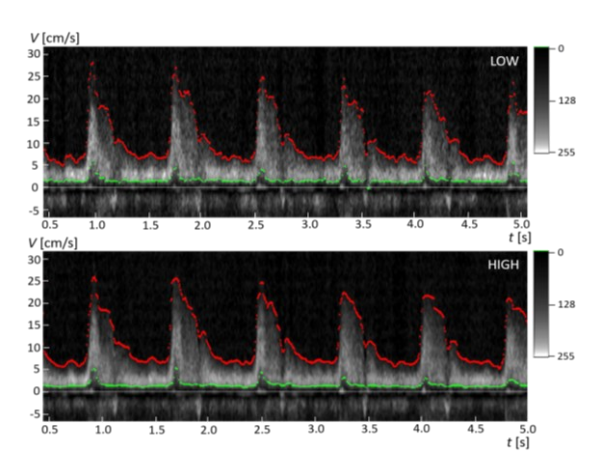
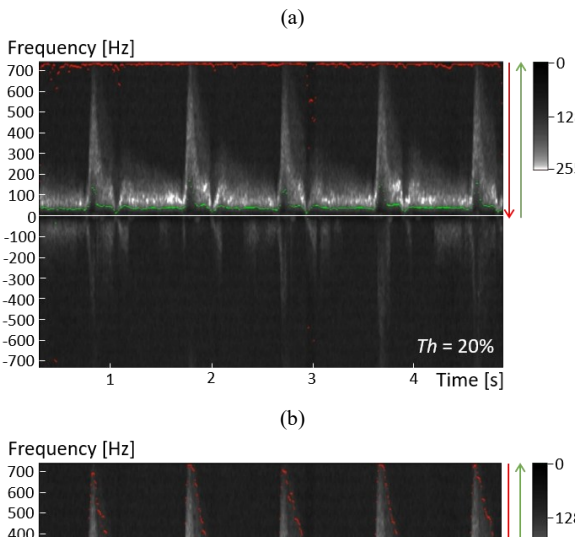
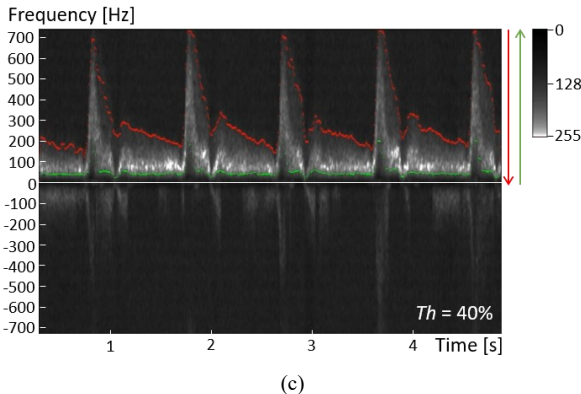


Fig. 8. Illustration of the envelope smoothing in the algorithm developed.

The degree of smoothing can be adjusted by the ultrasound machine user to improve the algorithm experience. Fig. 9 shows selected upper envelopes (Max - red) and lower envelopes (Min - green) of the blood flow velocity spectrum determined using the developed algorithm for several ranges of Th threshold values defined in percentages from 0 to 100%, where the 100% threshold refers to a pixel value = 255. The Doppler spectrum shown in Fig. 9 was recorded using the prototype of ultrasound B-mode scanner (Fig. 1) in the human common carotid artery in vivo.





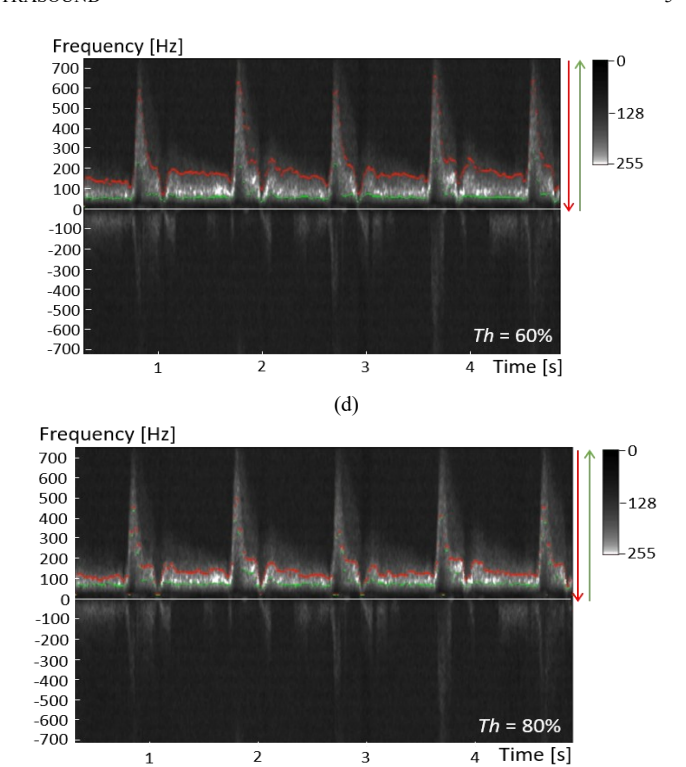


Fig. 9. Selected upper (red) and lower (green) envelopes of the common carotid artery blood flow velocity spectrum, determined using the developed algorithm for several threshold values defined in percent: Th = 20% (a), Th = 40% (b), Th = 60% (c), and Th = 80% (d). Arrows (red and green) indicate the direction in which to search for the pixel values in the lines for the upper and lower envelopes, respectively.

# C. Finding Characteristic Points and Indices of the Envelope

# 1) Points

The work also included the development of an algorithm for finding the most important characteristic points of the determined blood flow spectral envelope, as well as an algorithm for measuring heart rate (HR) based on the spectral analysis of the waveform envelope. The algorithm fully automatically determines the PSV (Peak Systolic Velocity), EDV (End Diastolic Velocity), and the point used to determine the AT (Acceleration Time) parameter (Fig. 10).

AT, also known as the time of contraction build-up, is an important indicator for predicting arterial stenosis (e.g., carotid or renal artery) or for estimating the overall impact of PAD (Peripheral Artery Disease), as it is strongly correlated with ankle or finger pressure indices.

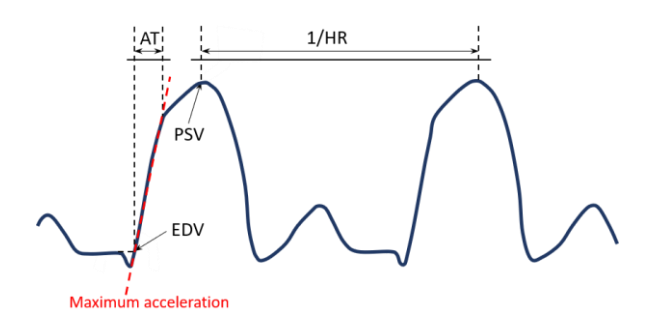


Fig. 10. Illustration of how to automatically determine the most important characteristic points of the flow velocity spectrum envelope.

AT may even become a new diagnostic criterion for critical limb ischemia [12]. Determining AT from the base of the envelope (EDV) to its maximum (PSV) is the easiest but imprecise. In the algorithm developed, it was decided to use measurements related to the first part of the upward slope of the envelope, that is, the maximum acceleration (Fig. 10), because such a value yields better results in detecting carotid and renal artery stenosis [13]-[17]. Moreover, the maximum acceleration at the very beginning of the systolic upward slope is not affected by reflected waves or other interfering factors.

### 2) Indices

Based on the characteristic points of the envelope of the blood flow spectral graph, algorithms have also been developed to determine indicators that parameterize the recorded blood flow velocity curves with a single number: the PI (Pulsation Index) and the RI (Resistance Index) [1],[4].

A quantitative assessment of the change in the shape of the blood flow velocity curve is defined in terms of the PI, which expresses the relationship between the harmonic components of the waveform [18]:

$$PI = \sum_{n=1}^{\infty} \frac{a_n^2}{a_n^2} \tag{9}$$

where  $a_n$  – the amplitude of the  $n^{th}$  harmonic,  $a_0$  – the average value of the curve. Thus, the PI index expresses the ratio of the energy contained in the oscillatory components to the constant component of the flow. The algorithm for determining PI was developed in a simplified way, determining the characteristic points of the envelope of blood flow velocity, using the formula [19]:

$$PI = \frac{V_{max} - V_{min}}{\bar{V}} \tag{10}$$

where  $V_{max}$  - maximum flow velocity,  $V_{min}$  - minimum flow velocity,  $\overline{V}$  – average flow velocity. With the increasing process of atherosclerotic lesions, a decrease in the pulsation of the curve is expected and, consequently, a decrease in the pulsation index. The pulsation index is independent of the frequency of the transmitted wave  $f_T$  and, importantly, is also independent of the angle  $\theta$  between the direction of propagation of the ultrasound wave and the axis of the blood vessel (Fig. 4). An example of how to determine the characteristic points of the blood flow velocity envelope to calculate the PI index is shown in Fig. 11 [20]. The blood flow velocity curve shows that the pulse wave and associated pulsatile blood flow change shape as it propagates along the vascular tree. The farther away from the heart, the smaller the pulsation and smoother the changes in the flow curve, while the constant component of the flow increases.

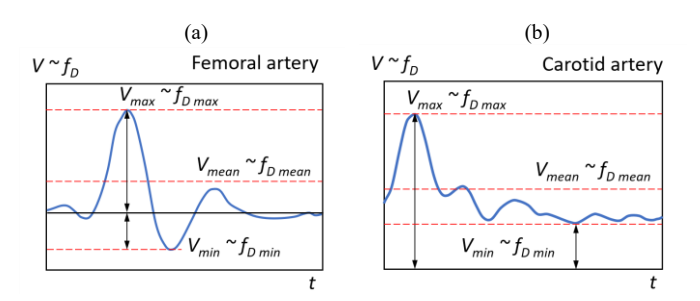


Fig. 11. Example of how to determine the characteristic points of the blood flow velocity envelope to calculate the PI index [20]: (a) carotid artery, (b) femoral artery.

The effect of elasticity and flow resistance on the blood flow velocity curves recorded at different locations is very important in the diagnosis of the blood circulation system. Based on the modelling, total blood flow in systole and diastole has been shown to be defined as the sum of the blood flow volume over time  $Q_A$  corresponding to the change in a rtic volume over time  $(dV_A/dt)$  and the volume of blood flow over time  $Q_n$  depending 

$$\frac{Systole}{Q_A} + \frac{Diastole}{Q_D} = C \cdot \frac{dP}{dt} + \frac{P}{R_D}$$
 (11)

where C – volumetric compliance of the blood vessel, P – instantaneous blood pressure. In the ascending aorta, the resistance is very high, so virtually no diastolic flow is observed there. The farther away the blood circuit, the more the diastolic component increases, as the flow resistances  $R_n$  decrease. An index related to vascular resistance in large blood vessels (especially in the carotid arteries) was proposed in the paper [21] as follows:

$$RI = \frac{(V_S)_{max} - V_D}{(V_S)_{max}}$$
 (12)

where  $(V_S)_{max}$  – maximum blood flow velocity in systole,  $V_D$  – maximum blood flow velocity in diastole. Using this formula, an algorithm was developed that determines the maximum systolic and diastolic blood flow velocity of the blood flow velocity envelope (Fig. 12).

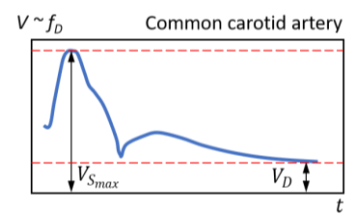


Fig. 12. Example of how to determine characteristic points of the common carotid artery blood flow velocity envelope to calculate the RI index [20].

According to the model (formula (11)), formula (12) assumes that the diastolic component of the flow is proportional to the instantaneous blood pressure and is responsible for the constant component of the flow, while the systolic component is related to the elasticity of the blood vessel under study. The systolic component is much higher in young people and decreases with age and with the increase of atherosclerotic lesions in the arteries. The RI in a normal common carotid artery takes values from 0.55 to 0.75. An increase in RI indicates a decrease in cerebral flow. An excessively low RI can indicate abnormal arteriovenous connections or arteriovenous malformations.

## III. RESULTS

The algorithm for Doppler imaging of blood flow in PWD mode with automatic determination of the envelope of the flow velocity spectrum and measurement of flow parameters was implemented in the prototype ultrasound B-mode scanner developed within the framework of the research project. PWD imaging tests were performed on an appropriately programmed ATS Cardiac Doppler Flow Phantom Model 523 [22] stimulated with a Doppler Flow Pump Model 769 [2] filled with Doppler Fluid Model 769DF [3] (Fig. 13).

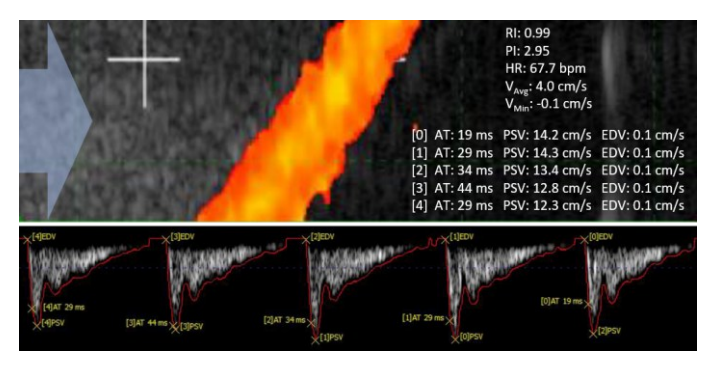


Fig. 13. An example of the performance of the developed CFM+PWD Doppler imaging algorithm implemented in the prototype 128-channel ultrasound B-mode scanner.

#### IV. DISCUSSION

Table I lists the characteristic values of EDV, PSV and AT parameters for 5 cycles of pulsed flow, determined automatically from the maximum flow velocity envelope shown in Fig. 13, along with the percentage deviations from the average value.

TABLE I

CHARACTERISTIC VALUES AND THEIR SPREAD AUTOMATICALLY DETERMINED FROM THE ENVELOPE OF THE FLOW SPECTRUM FROM FIG. 13

EDV <sub>i</sub> [cm/s]	$\frac{\overline{\text{EDV}_i} - \overline{\text{EDV}}}{\overline{\text{EDV}}}$ [%]	PSV <sub>i</sub> [cm/s]	$\frac{\overline{PSV_i} - \overline{PSV}}{\overline{PSV}}$ [%]	AT [ms]	$\frac{AT_i - \overline{AT}}{\overline{AT}}$ [%]
0.1	0.0	14.2	+6.0	19	-38.7
0.1	0.0	14.3	+6.7	29	-6.5
0.1	0.0	13.4	0.0	34	+9.7
0.1	0.0	12.8	-4.5	44	+41.9
0.1	0.0	12.3	-8.2	29	-6.5

The standard deviations of this sample determined for particular parameters are:  $\sigma(EDV) = 0.00 \text{ cm/s}$ ,  $\sigma(PSV) = 0.87 \text{ cm/s}$ ,  $\sigma(AT)$ = 9.08 ms, respectively. The highest reproducible determination accuracy was obtained for the EDV parameter, followed by PSV, demonstrating the suitability of the developed method for determining the PI and RI indices and using them in diagnostic studies. The largest spread occurred for the AT parameter, which in turn is in line with predictions. Pulsatile flow generated by a peristaltic pump, such as blood flow in blood vessels, exhibits velocity fluctuations, which affects the shape of the upper and lower envelopes of the blood flow velocity. For this reason, a correctly determined envelope should not show significant deviations in the EDV and PSV measurements; however, extreme variations in the AT measurements based on the slope of maximum acceleration at the very beginning of the systolic upward slope can be expected.

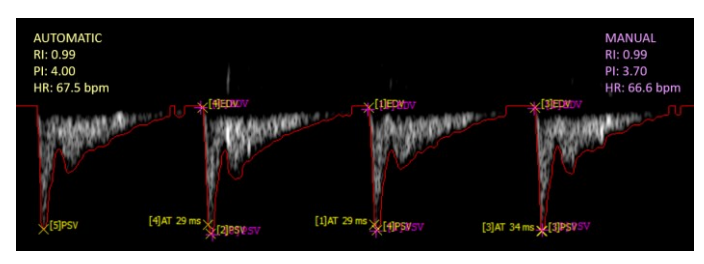


Fig. 14. Results of a PWD imaging test performed on an ATS Cardiac Doppler Flow Phantom Model 523 [22] comparing automatic (yellow) and manual (purple) determination of flow parameters.

The test results showed  $\pm$  10% accuracy in volume measurement relative to manual measurement, as well as measurement of blood flow parameters with  $\pm$  10% accuracy relative to manual measurement, for the parameters: PSV, EDV, mean velocity, RI, and PI coefficients (Fig. 14).

#### V. CONCLUSIONS

As a result of the tests, the performance of the method developed for automatic calculation of the envelope of the blood flow velocity curve in spectral Doppler imaging was sufficiently good in terms of repeatability and precision. The low computational complexity of the algorithm developed, which was implemented in the prototype 128-channel ultramobile ultrasound B-mode scanner, means that it does not burden the memory resources and FPGAs used for the device and is fast in operation.

#### REFERENCES

- W. Schäberle, "Ultrasonography in Vascular Diagnosis", Springer-Verlag, 2011. https://doi.org/10.1007/978-3-642-02509-9
- [2] Doppler Flow Pump Model 769, User Guide, Sun Nuclear. https://www.sunnuclear.com/uploads/documents/datasheets/769-DS-090723-1.pdf
- [3] Doppler Fluid Model 769DF, User Guide, Sun Nuclear. https://www.sunnuclear.com/uploads/documents/datasheets/769-DS-072220-1.pdf
- [4] A. Nowicki, "Ultrasonografia wprowadzenie do obrazowania i metod dopplerowskich", Wydawnictwo IPPT PAN, Warszawa, 2016 (in Polish).
- [5] G. Fiori, F. Fuiano, A. Scorza, et al., "Doppler Flow Phantom Stability Assessment through STFT Technique in Medical PW Doppler: a preliminary study", presented at 2021 IEEE International Workshop on Metrology for Industry 4.0 & IoT Conference, Rome, June 07-09, 2021. https://doi.org/10.1109/MtroInd4.0IoT51437.2021.9488513
- [6] I.B. Gonçalves, A. Leiria, M.M.M. Moura, "STFT or CWT for the detection of Doppler ultrasound embolic signals", International Journal for Numerical Methods in Biomedical Engineering vol. 29, pp. 964-976, 2013. https://doi.org/10.1002/cnm.2546
- [7] L.R. Rabiner, R.W. Schafer, "Digital processing of speech signals", Prentice Hall, Englewood Cliffs, New Jersey, 1978.
- [8] L.R. Rabiner, R.W. Schafer, "Introduction to digital speech processing", now Publishers Inc., Boston-Delft, 2007.
- [9] J.B. Allen and L.R. Rabiner, "A unified approach to short-time Fourier analysis and synthesis," in Proc. of the IEEE , vol. 65, pp. 1558-1564, 1977. https://doi.org/10.1109/PROC.1977.10770
- [10] K.-J. Wolf, F. Fobbe, "Color Duplex Sonography, Principles and Clinical Applications", Thieme Medical Publishers, New York, 1995.
- [11] J.B. Elsner, A.A. Tsonis, "Singular Spectrum Analysis. A New Tool in Time Series Analysis", Springer New York, New York, 1996. https://doi.org/10.1007/978-1-4757-2514-8
- [12] J.-E. Trihan, G. Mahé, J.-P. Laroche, et al., "Arterial Blood-Flow Acceleration Time on Doppler Ultrasound Waveforms: What Are We Talking About?", Journal of Clinical Medicine, vol. 12, no. 3, 2023. https://doi.org/10.3390/jcm12031097
- [13] K. Iizuka, H. Takekawa, A. Iwasaki, et al., "Suitable methods of measuring acceleration time in the diagnosis of internal carotid artery stenosis", Journal of Medical Ultrasonics, vol. 40, pp. 327-333, 2020. https://doi.org/10.1007/s10396-019-01000-x
- [14] M. Bardelli, F. Veglio, E. Arosio, et al., "New intrarenal echo-Doppler velocimetric indices for the diagnosis of renal artery stenosis", Kidney International, vol. 69, pp. 580-587, 2006. https://doi.org/10.1038/sj.ki.5000112
- [15] J.J.W.M. Brouwers, J.F.Y. Jiang, R.T. Feld, et al., "A New Doppler-Derived Parameter to Quantify Internal Carotid Artery Stenosis: Maximal Systolic Acceleration", Annals of Vascular Surgery, vol. 81, pp. 202-210, 2022. https://doi.org/10.1016/j.avsg.2021.09.056
- [16] J.J.W.M. Brouwers, L.P. van Doorn, L. Pronk, et al., "Doppler Ultrasonography Derived Maximal Systolic Acceleration: Value

- Determination with Artificially Induced Stenosis", Vascular and Endovascular Surgery, vol. 56, pp. 472-479, 2022.
- https://doi.org/10.1177/15385744221076269
- [17] J.J.W.M Brouwers, L.P. van Doorn, R.C. van Wissen, H. Putter, J.F. Hamming, "Using maximal systolic acceleration to diagnose and assess the severity of peripheral artery disease in a flow model study", Journal of Vascular Surgery, vol. 71, pp. 242-249, 2020.
  - https://doi.org/10.1016/j.jvs.2019.01.088
- [18] R. Gosling, F. Dunbar, D. King, et al. "The quantitative analysis of occlusive peripheral arterial disease by a non-intrusive technique", Angiology, vol. 22, pp. 52-55, 1971.
  - https://doi.org/10.1177/000331977102200109

- [19] R. Gosling, D. King, "Continuous wave ultrasound as an alternative and complement to X-rays in vascular examination", in Cardiovascular Applications of Ultrasound, chapter 22, R.S. Reneman Ed., Amsterdam: North-Holland, pp. 266-282, 1974.
- [20] A. Nowicki, "Podstawy ultrasonografii dopplerowskiej". Wydawnictwo Naukowe PWN, Warszawa, 1995 (in Polish).
- [21] C.W.L. Pourcelot, "Doppler techniques in cerebral vascular disturbances", in Doppler Ultrasound in the Diagnosis of Cerebrovascular Disease, R. Reneman and A. Hoeks Ed., Chichester: Research Studies Press, 1982.
- [22] ATS Cardiac Doppler Flow Phantom Model 523, User Guide, Sun Nuclear
  - $https://www.sunnuclear.com/uploads/documents/datasheets/ATS523APh \ antom \ 0080522.pdf$